

Communication

Polarization Potential Has No Effect on Maximum Current Density Produced by Halotolerant Bioanodes

Muriel González-Muñoz ¹, Xochitl Dominguez-Benetton ², Jorge Domínguez-Maldonado ¹, David Valdés-Lozano ³, Daniella Pacheco-Catalán ¹ , Otto Ortega-Morales ⁴ and Liliana Alzate-Gaviria ^{1,*}

¹ Energía Renovable, Centro de Investigación Científica de Yucatán (CICY), Km 5 Carretera Sierra Papacal-Chuburná Puerto, Yucatán 97302, Mexico; murielgonzalez@cicy.mx (M.G.-M.); joe2@cicy.mx (J.D.-M.); dpacheco@cicy.mx (D.P.-C.)

² Separation and Conversion Technology, Flemish Institute for Technological Research (VITO), Boeretang 200, 2400 Mol, Belgium; xoch@vito.be

³ Departamento de Recursos del Mar, Centro de Investigación y Estudios Avanzados del Instituto Politécnico Nacional (CINVESTAV-Mérida), Km 6 Antigua Carretera a Progreso, Yucatán 97310, Mexico; dvaldes@cinvestav.mx

⁴ Departamento de Microbiología Ambiental y Biotecnología, Universidad Autónoma de Campeche (UACAM), Av. Agustín Melgar S/N, Col. Buenavista, Campeche 24039, Mexico; beortega@uacam.mx

* Correspondence: lag@cicy.mx; Tel.: +52-999-930-0760

Received: 7 December 2017; Accepted: 23 February 2018; Published: 1 March 2018

Abstract: Halotolerant bioanodes are considered an attractive alternative in microbial electrochemical systems, as they can operate under higher conductive electrolytes, in comparison with traditional wastewater and freshwater bioanodes. The dependency between energetic performance and polarization potential has been addressed in several works; however the vast majority discusses its effect when wastewater or freshwater inocula are employed, and fewer reports focus on inocula from highly-saline environments. Moreover, the effect of the polarization potential on current production is not fully understood. To determine if the polarization potential has a significant effect on current production, eight bioanodes were grown by chronoamperometry at positive and negative potentials relative to the reference electrode (+0.34 V/SHE and −0.16 V/SHE), in a three-electrode set-up employing sediments from a hyperhaline coastal lagoon. The maximum current density obtained was the same, despite the differences in the applied potential. Our findings indicate that even if differences in organic matter removal and coulombic efficiency are obtained, the polarization potential had no statistically significant effect on overall current density production.

Keywords: polarization potential; halotolerant bioanodes; microbial electrochemical systems

1. Introduction

Microbial electrochemical systems (MES) have become highly attractive as they provide a robust platform of valuable chemicals (biofuels, organic acids, metals, etc.), removal of pollutants (nitrobenzene, chlorophenol, hexavalent chromium, etc.), and biosensors, in a sustainable manner [1–3]. Such electrochemical devices employ microorganisms as catalysts, which are often anaerobic bacteria forming an electroactive biofilm. In most cases, these bacteria oxidize organic matter by an anodic reaction, to produce an electric current that drives a cathodic reaction (biocatalyzed or not), through which the main chemicals of interest are produced [4,5].

An important disadvantage in comparison to more classical electrochemical systems is that MES usually work with low conductivity electrolytes (<20 mS cm^{−1}), resulting in high Ohmic drops that lead

to significant energy losses [6,7]. Even with the current output improvements achieved with multilayer bioanode structures [6], the overall incapability of the commonly used microbial biomass to tolerate highly conductive electrolytes makes them unattractive for most energy-demanding applications [5,8]. Thus, electrolyte conductivity should be as high as possible to develop more competitive MES [9].

It has been demonstrated that an increase in electrolyte conductivity in MES enhances current and power outputs as the internal resistance decreases [6,7]. However, this improvement in performance is possible only if the salt concentration in the electrolyte is maintained below the tolerance threshold of anodic microorganisms [7]. When this threshold is surpassed, bacteria are inhibited by osmotic pressure [9,10], and impairment in the energy performance is expected, despite further conductivity increments. So far, a maximum salt concentration of 25 to 35 g L⁻¹ (up to 55 mS cm⁻¹) is tolerated when freshwater microorganisms are employed as inoculum [11–14], given that they are not naturally adapted to saline environments. Marine sediments and sea water (about 35 g L⁻¹ and 54 mS cm⁻¹) have been reported as a microorganism source in MES, but mostly in sediment microbial fuel cells, which are characteristic of poor energetic performances (0.005–1.100 A m⁻² and 0.003–0.400 W m⁻²) [15–17]. Moreover, fewer reports discuss the use of marine microorganisms in typical MES configurations, with better current outputs, up to 8.20 A m⁻² [10,18]. In recent years, the use of halophile and halotolerant bacteria as a biocatalyst in MES was proposed with promising results [7,19]. These bacteria are adapted to salt concentrations in an interval of 30–300 g L⁻¹ [20,21], which corresponds to approximately 50–450 mS cm⁻¹ [22]. It is important to note that an additional advantage to MES of using high salinity media is the intrinsic inhibition of methanogenic bacteria [6], which in many instances counteract the efficiency of conversions to electric energy or other value-added chemicals.

Halophile and halotolerant microbes are characterized for the production of exopolymeric substances (biofilm formers) and extracellular proteins [23,24], which, in turn, may act as natural mediators for electron transfer [25,26]; such attributes make them attractive as catalysts in MES. A maximum current density of 85 A m⁻² has been reported with a salt marsh inoculum [7], wherein a stringent selection of microorganisms at the bioanode was achieved through a constant polarization potential. A well-colonized bioanode mainly dominated by *Marinobacter* spp. and *Desulfuromonas* spp. has been observed at 104 mS cm⁻¹, after 15 to 25 days of growth [27]. Nevertheless, more modest performances are frequently obtained with microorganisms from highly saline environments, about 0.3 to 20 A m⁻², and species belonging to the genera *Marinobacter*, *Geobacter*, *Chlorobium*, *Clostridium*, *Rhodospseudomonas*, *Pelobacter*, *Desulfobulbus*, *Desulfocapsa*, *Halanaerobium*, *Halomonas*, *Aeromonas*, *Natrialba*, and *Haloferax* [8,19,28–32]. It is noteworthy that anode-colonizing species at elevated salt concentrations may differ from freshwater anode species or not, suggesting that saline environments are an interesting source of unknown electroactive bacteria, as well as a source of known electroactive microorganisms that are naturally adapted to highly saline conditions. On the other hand, the relationship between current density and the anode polarization potential has been previously discussed, but with many discrepancies between works. In some cases, the overall energetic performance was enhanced at higher polarization potentials [8,33,34]. Meanwhile, bioanodes polarized at more negative potentials showed better performance according to other authors [35,36]. Also, no dependence between the polarization potential and energetic performance has been reported [37]. Such discrepancies may be explained by differences in inoculum selection, electrolyte conductivity, anode-supporting material, cell configuration, nutrient availability, and carbon source type [37–39]. Furthermore, some evidence points to the effect of the polarization potential over current density, which is different for each inoculum [39].

Enrichment of electroactive bacteria by a constant polarization potential in a three-electrode cell configuration has some advantages over closed circuit with resistor enrichment (two-electrode cell configuration): with the later, current production is limited not only by a selective exoelectrogenic activity and substrate availability. Conversely, when a resistive load is imposed in two-electrode configuration, the anodic potential is not fixed but variable, directly affecting the overall current production [40].

Since halotolerant bioanode development is a recent field of research, further investigations are required to determine the most convenient polarization potential at elevated electrolytic conductivity, to boost their energetic performance. The aim of this study was to determine if variations in current density are governed by the polarization potential when exoelectrogenic bacteria are enriched under constant polarization potential employing sediments from a hyperhaline coastal lagoon as inoculum. To achieve this goal, eight bioanodes were grown by chronoamperometry at positive and negative polarization potential versus standard hydrogen electrode (four at +0.34 V/SHE and four at −0.16 V/SHE, respectively) under elevated salinity conditions.

2. Materials and Methods

2.1. Inoculum and Medium

Superficial sediments (approx. first 40 cm) were collected from the hyperhaline coastal lagoon “Ría Lagartos,” located in Yucatán, México. Samples were collected in triplicate with a 5 L capacity dredge, in the vicinity of a solar saltwork (Las Coloradas 21°34' N, 87°57' O). The water conductivity, salinity, dissolved oxygen, and pH of the water column was measured in situ with an YSI ProPlus (YSI Incorporated, Yellow Springs, OH, USA) multi-parameter instrument and probes. Sediment temperature, pH, and redox potential were measured with Extech (Extech Instruments, Boston, MA, USA) portable electrodes (ExtStik PH110 and ExtStik RE300). Additionally, the volatile solids concentration in the sediment was measured by gravimetric methods [41] in order to further estimate the inoculum size, in terms other than just the volume ratio; the effective volatile solid concentration in the sediment was of 103.63 ± 12.96 mg per gram of sediment. The culture medium [7,8,27,39,42] was prepared as follows: NH_4Cl 2 g L^{-1} , K_2HPO_4 0.5 g L^{-1} , sodium acetate 3.6 g L^{-1} (40 mM), $\text{MgCl}_2 \cdot 6\text{H}_2\text{O}$ 55 mg L^{-1} , 1 mL L^{-1} of metal solution (HCl 37% 46 mL L^{-1} , $\text{FeSO}_4(\text{NH}_4)_2\text{SO}_4 \cdot 6\text{H}_2\text{O}$ 7 g L^{-1} , $\text{ZnCl}_2 \cdot 2\text{H}_2\text{O}$ 1 g L^{-1} , $\text{MnCl}_2 \cdot 4\text{H}_2\text{O}$ 1.2 g L^{-1} , $\text{CuSO}_4 \cdot 5\text{H}_2\text{O}$ 0.4 g L^{-1} , $\text{Mo}_7\text{O}_2(\text{NH}_4)_6 \cdot 4\text{H}_2\text{O}$ 1 g L^{-1} , $\text{NiCl}_2 \cdot 6\text{H}_2\text{O}$ 0.05 g L^{-1} and $\text{Na}_2\text{SeO}_3 \cdot 5\text{H}_2\text{O}$ 0.01 g L^{-1}), $\text{CaCl}_2 \cdot 2\text{H}_2\text{O}$ 60 mg L^{-1} and 50 g L^{-1} of NaCl. The pH was adjusted to 7.9 with 1 M NaOH. Aliquots of 170 mL of culture medium were transferred into 250 mL Erlenmeyer flasks, supplemented with 30 mL of sediment (15 vol %), corresponding to a calculated final concentration of circa 26,357 mg of volatile solids per liter). The liquid and headspace were flushed with N_2 gas for 20 min to reduce dissolved oxygen concentration in the liquid, and the content was transferred by the Hungate technique [43] to the electrochemical cell (see Section 2.2). The cell was sealed with a prefabricated cap and butyl rubber stoppers, until the sediments settled in the bottom [38]. After that, three of the four stoppers were removed and the working, auxiliary, and reference electrodes were placed instead. The fourth stopper was used as a sampling port. Final conductivity, dissolved oxygen, and pH after inoculation were measured with a HQ40D Portable Multi Meter (Hach Company, Loveland, CO, USA). Also, chemical oxygen demand (COD) was quantified with a low range COD Digestion Vial Kit (Hach Company, Loveland, CO, USA), diluting the samples 40 times by two successive dilutions (1:10 and 1:4) in ultrapure water. Each sample was independently taken from each cell using a syringe through the sample port, at a midpoint distance of the bottom, in order to avoid the resuspension of settled sediments. The sample was immediately diluted as described, digested in a DRB200 reactor (Hach Company, Loveland, CO, USA) and read in a DR1900 Portable Spectrophotometer (Hach, Company, Loveland, CO, USA) following the manufacturer's instructions.

2.2. Electrochemical Set-Up

A three-electrode set-up was assembled in a prefabricated borosilicate electrochemical cell, with a working volume of 200 mL. The working electrode consisted of 7 cm^2 (projected surface area) of AvCarb G200 carbon felt (Fuel Cell Store, College Station, TX, USA) with a platinum wire (10 cm long and \varnothing of 0.5 mm, Merck KGaA, Darmstadt, Hesse, Germany) as the electrical collector. A graphite rod of 17.25 cm^2 (projected surface area) was used as the auxiliary electrode, and a saturated calomel

electrode (+0.24 V/SHE) as the reference. The working and auxiliary electrodes were set 3 cm away from each other. None of the electrodes made direct contact with the sediment inoculated and settled in the bottom of the cell.

2.3. Bioanode Growth and Electrochemical Characterization

Eight bioanodes were independently grown by chronoamperometry with a Bio-Logic VPS potentiostat (Bio-Logic Science Instruments, Seyssinet-Pariset, Grenoble, France), setting the potential value of the working electrodes at two different magnitudes: four bioanodes at +0.34 V/SHE and four at −0.16 V/SHE, correspondingly. The four bioanodes grown at each polarization potential are referred to as Run #1, Run #2, Run #3, and Run #4 all through the figures, tables, and text. The constant electric polarization was sustained for 21 days, which is long enough to obtain a colonized bioanode on carbon electrodes by marine and salt marsh exoelectrogenic bacteria [7,8,27,44], yet presumably insufficient to fully stabilize the microbial succession [45]. The current response was recorded every hour. The system remained unagitated throughout the experiment. Current production mean by day was calculated and normalized with respect to the anode projected surface area. The COD was measured regularly, as described in Section 2.1. Acetate was fed into the cell every three to five days to avoid microbial starvation [7]. The quantity of electric charge produced by each bioanode was calculated by integrating the area under the chronoamperometric curve with respect to time. The coulombic efficiency and power density were calculated according to Logan [46,47]. Conductivity, dissolved oxygen, and pH were monitored during the experiment with the HQ40D Portable Multi Meter (Hach Company, Loveland, CO, USA). At the end of each run, the electrochemical cell was disconnected and, after reaching relaxation, the open circuit potential (OCV) of the anode was measured. A linear voltammetry was recorded from the OCV to an overpotential of at least 1 V (~0.740 V/SHE) at 1 mV s^{−1}. A cyclic voltammetry was performed under the same conditions right after the inoculation (at day 0) for all eight cells, in order to evaluate the background contribution on current density of the overall chemical redox species and original microbial community carried within the inoculum.

2.4. Statistical Analysis

To validate our observations, an analysis of variance (ANOVA Fisher Test, with $\alpha = 0.10$ and $\alpha = 0.05$) was made to compare the values obtained at each applied potential with Minitab 17 software (Minitab Incorporated, 2017, State College, PA, USA). The results of this analysis are indicated as superindexes along the text and tables, next to mean values and their standard deviation. The same letter indicates that no significant difference was found between the treatments (+0.34 V/SHE and −0.16 V/SHE applied polarization potential, respectively).

3. Results

3.1. Inoculum and Medium Characterization

The conductivity and salinity of the water column at the collection site were 73.35 ± 3.34 mS cm^{−1} and 50.44 ± 2.59 g L^{−1}, respectively. Temperature, pH, and dissolved oxygen concentration values of 31.70 ± 0.60 °C, 7.92 ± 0.10 pH units, and 4.72 ± 0.72 mg O₂ L^{−1} were measured, correspondingly. The temperature, pH, and redox potential values from the sediment samples collected were 30.32 ± 1.56 °C, 6.95 ± 0.24 , and -0.28 V/SHE, respectively. After culture medium inoculation, a final conductivity of 67.12 ± 2.84 mS cm^{−1} and a pH of 7.73 ± 0.24 were registered. The initial COD concentration was 2400 ± 150 mg L^{−1}.

3.2. Bioanode Growth and Current Production

Current density versus time plots for the positive (+0.34 V/SHE) and negative (−0.16 V/SHE) polarization potential are shown in Figure 1. Current production was observed first at the negative potential (except for Run #4), after two or three days of polarization, in comparison to the positive

potential, where current production was registered only at day 5 for all four runs. This suggests that the electroactive community developed faster at the polarization potential of -0.16 V/SHE, as significant differences were found by ANOVA analysis between polarization potentials during the first five days of polarization. This is in agreement with the results of Torres et al. [36], who observed a faster start-up at lower potentials when marine sediments were used as inoculum, but contrasts with other reports where higher potentials promoted a faster start-up, for *Shewanella oneidensis* axenic cultures [42] and domestic wastewater mixed inoculum [48]. Remarkably, as in this report, the current performance at the end of the experiments was almost the same, regardless of the applied potential or if the start-up occurred first or not. After 10 days of polarization and until the end of the experiment, the mean current density showed no significant differences in spite of the applied potential. Likewise, high standard variation was observed. During that period, mean values of 1.09 ± 0.59^a and 1.06 ± 0.61^a A m^{-2} were recorded at $+0.34$ V/SHE and -0.16 V/SHE, respectively. Maximum current density peaks were reached after 16 days of polarization in all cases. The values for all experimental runs are shown in Table 1. The highest values registered were 2.64 A m^{-2} at $+0.34$ V/SHE (Run #1) and 2.45 A m^{-2} at -0.16 V/SHE (Run #4). No significant differences in maximum current density between applied potentials were found. No statistical difference in electric charge production through 21 days of polarization was observed either, which was of 346.25 ± 130.94^a C and 476.44 ± 300.74^a C, for positive and negative potentials, respectively. This was consistent with results reported by Zhou et al. [37], who found that even if each experimental unit showed differences in current density, in the end, the quantity of coulombs delivered by each bioanode was the same regardless of the potential applied during the biofilm growth.

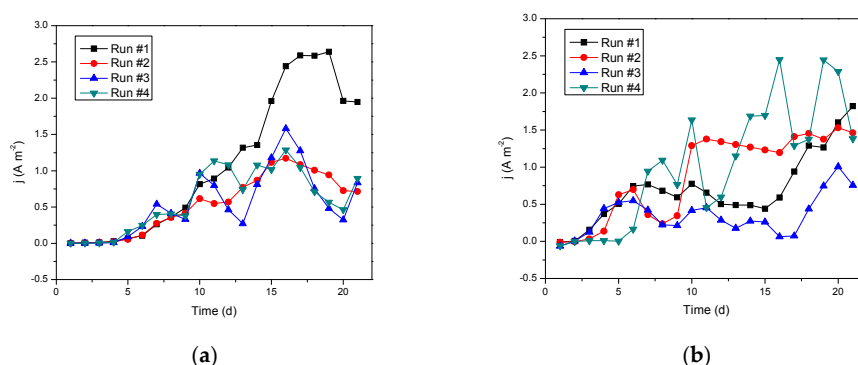


Figure 1. Current density versus time at (a) $+0.34$ V/SHE and (b) -0.16 V/SHE polarization potential.

Table 1. Maximum current density recorded at $+0.34$ V/SHE and -0.16 V/SHE polarization potentials.

Polarization Potential	Maximum Current Density (A m^{-2})				
	Run #1	Run #2	Run #3	Run #4	Mean
$+0.34$ V/SHE	2.64 (day 19)	1.17 (day 16)	1.58 (day 16)	1.29 (day 16)	1.67 ± 0.67^a
-0.16 V/SHE	1.82 (day 21)	1.53 (day 20)	1.07 (day 20)	2.45 (day 16)	1.72 ± 0.58^a

^a Letters as subindexes indicate the results obtained by the ANOVA.

The OCV of the anode was more variable at negative potential (-0.243 V/SHE, -0.246 V/SHE, -0.273 V/SHE and -0.292 V/SHE, for each run) than at the positive one (-0.287 V/SHE, -0.292 V/SHE, -0.275 V/SHE and -0.294 V/SHE, for each run). Mean values of $-0.263.50 \pm 0.023^a$ V/SHE and $-0.287.00 \pm 0.008^a$ V/SHE were registered, respectively, with no statistical differences. This suggests that the OCV is dependent of the carbon source, acetate in this case, which has a standard reduction potential of -0.298 V/SHE ($\text{pH} = 7$, 50 mM $\text{CH}_3\text{COO}^- + 2\text{H}_2\text{O} \rightarrow 2\text{CO}_2 + 7\text{H}^+ + 8\text{e}^-$) [49], as it has been previously observed [8]. Those values are shown in Table 2. The highest maximum power densities were registered at day 19 and 16 for $+0.34$ V/SHE and -0.16 V/SHE, which corresponded to 1.39 W m^{-2} (Run #1) and 1.27 W m^{-2} (Run #4), respectively.

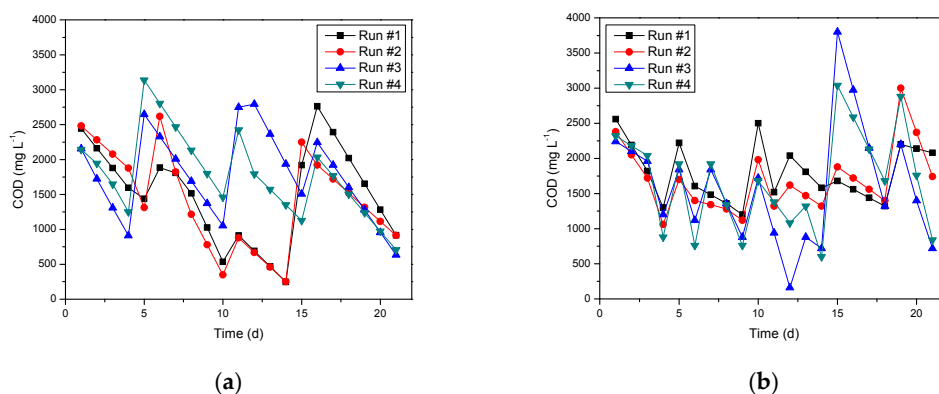
Table 2. Maximum power density recorded at +0.34 V/SHE and −0.16 V/SHE polarization potentials.

Polarization Potential	Maximum Power Density ($W m^{-2}$)				
	Run #1	Run #2	Run #3	Run #4	Mean
+0.34 V/SHE	1.39 (day 19)	0.62 (day 16)	0.77 (day 16)	0.64 (day 16)	0.85 ± 0.36^a
−0.16 V/SHE	0.88 (day 21)	0.77 (day 20)	0.55 (day 20)	1.27 (day 16)	0.88 ± 0.30^a

^a Letters as subindexes indicate the results obtained by the ANOVA.

The coulombic efficiencies reached at the end of the experiments were in the range of 7% to 16% at +0.34 V/SHE, and between 13% and 53% for −0.16 V/SHE. These values were comparable to those reported by Rousseau et al. [5] (between 2% and 25%), who used a very similar inoculum source to ours, similar materials, carbon source, medium composition, and conductivity. More elevated coulombic efficiencies were reached at the negative potential in comparison with the positive one, which are consistent with other reports, where the conductivity was less than 50 mS cm^{-1} and the microorganisms employed were obtained from brackish or freshwater streams [10,11,34]. The percentage achieved at −0.16 V/SHE ($29.89 \pm 17.01^b\%$) was superior with respect to that reached at +0.34 V/SHE ($10.58 \pm 4.41^a\%$), with marginal significance. This means that a statistical difference in the coulombic efficiency was found at a confidence interval of 10% ($\alpha = 0.10$) but not at 5% ($\alpha = 0.05$). Coulombic efficiency values obtained at the negative potential were similar to those reported by Lefebvre et al. [10] (20% to 60%) and Liu et al. [11] (20% to 60%), where wastewater was used as inoculum in a microbial fuel cell, and NaCl concentration in the electrolyte was between 0 and 40 g L^{-1} , and between 6 and 23 g L^{-1} , respectively [10,11].

COD consumption and feeding profiles are presented in Figure 2. COD removal percentage was greater at positive polarization potential, in the range of 55% to 74%, in comparison to the 36% to 57% obtained at the negative potential. Significant differences were detected between means, which were $66.12 \pm 8.03^a\%$ and $47.86 \pm 10.37^b\%$, respectively. Superior COD removal at positive potential may be caused by a more diverse anodic community, capable of using other biochemical pathways different than anode respiration [32,36], which is consistent with lower coulombic efficiency values.

**Figure 2.** COD consumption and feeding profiles during chronoamperometry at (a) +0.34 V/SHE and (b) −0.16 V/SHE polarization potential.

The electrolyte conductivity was maintained between 63 and 74 mS cm^{-1} throughout this study. Dissolved oxygen concentration was always below 2.5 mg L^{-1} in all the experiments; pH values in the electrolyte were maintained in the range of 7.2 to 8.2 units in all eight experiments. A good natural buffer capacity was observed, as the pH slightly decreased after acetate feeding and then it was rapidly restored to slightly alkaline values (around 7.8) before acetate was consumed. This is explained by the large inoculum size employed in this study (15 vol %) and the high concentration of carbonates present in the sediments, as is typical at the site of sample collection because of the calcareous nature of the soil [46].

3.3. Maximum Current Density by Linear Voltammetry

At the end of each run, the chronoamperometry was stopped, and a linear voltammetry was performed after the OCV was stabilized. The results for each run are presented in Figure 3. The current contribution of chemical redox chemical species carried in the inoculum (other than acetate degradation) was discarded, as the eight voltammeteries performed at day 0 did not show significant oxidative current density ($<0.1 \text{ A m}^{-2}$) within the scanned potential interval. Current onset was reached first when the polarization potential of -0.16 V/SHE was applied during electroactive biofilm growth, where three of four runs showed an oxidative current as soon as the voltammetry began, which corresponds to an overvoltage between 0 and 0.05. The only exception was observed in run #2, where the onset was detected at an overvoltage above 0.1 V. Concerning the bioanodes grown at a polarization potential of $+0.34 \text{ V/SHE}$, all runs showed an oxidative current when an overvoltage above 0.05 V was applied. Like in chronoamperometry, current density values were quite variable between runs, in spite of the applied potential during biofilm growth. Also, variations in oxidative current peaks were observed between each run, raising the possibility that different oxidation processes occur even at the same polarization potential, which is representative of diverse redox proteins and microbial species at the anode surface. This is evident in Figure 3, where Run #1, Run #2, and Run #4 showed very similar voltamperometric shapes for each independent polarization potential. Also, Run #3 at both polarization potentials ($+0.34 \text{ V/SHE}$ and -0.16 V/SHE) showed similar patterns but was different from the first group (Run #1, Run #2, and Run #4) for each polarization potential. As every experimental run was done separately, similarities or dissimilarities in current profiles due to possible experimental variations should be discarded. It should be noted that maximum current density was achieved above an overvoltage of 0.60 V in all cases, except for Run #3 at negative potential, where maximum current density was obtained at 0.3 V. These values are presented in Table 3, and are substantially higher than those obtained by chronoamperometry (Table 1). Despite the more pronounced increment in current at lower overvoltages, apparently observed at -0.016 V/SHE polarization, the difference in maximum current density values between applied polarization potentials was not statistically significant. It is important to notice that current density differences at lower overvoltages may change over time, as was observed by Lewis et al. [35], who reported a significant shift in midpoint potential between two pre-enriched biofilms polarized at $+0.20 \text{ V/SHE}$ and -0.20 V/SHE . Their results showed that a biofilm polarized at negative potential (-0.20 V/SHE) produces higher current densities at lower potentials in comparison with a positive one ($+0.20 \text{ V/SHE}$), but this was clearly observable after three months of polarization. Thus, an interesting question to ask would be whether the bioanodes obtained here are subjected to the same phenomenon if longer evaluation periods are addressed.

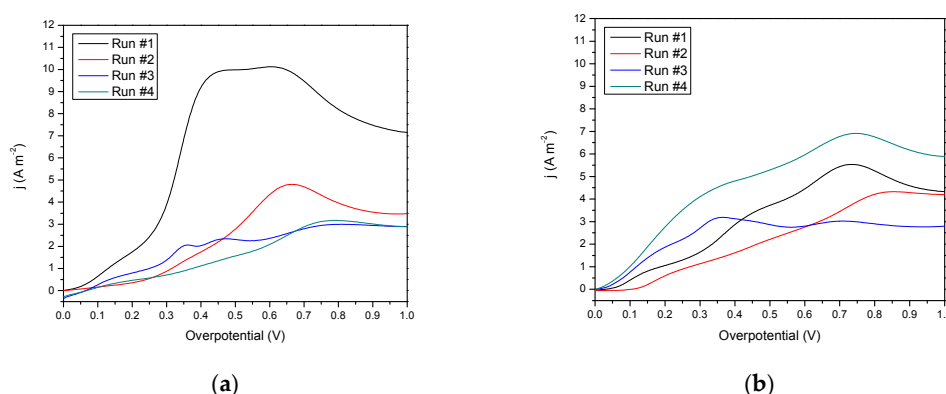


Figure 3. Linear voltammetry (1 mV s^{-1}) after 21 days of polarization at (a) $+0.34 \text{ V/SHE}$ and (b) -0.16 V/SHE .

Table 3. Maximum power density recorded by linear voltammetry after 21 days of polarization at +0.34 V/SHE and −0.16 V/SHE potential.

Polarization Potential	Maximum Current Density (A m^{-2})				
	Run #1	Run #2	Run #3	Run #4	Mean
+0.34 V/SHE	10.12	4.80	3.00	3.17	5.27 ± 3.38^a
−0.16 V/SHE	5.54	4.32	3.18	6.91	4.99 ± 1.60^a

4. Discussion

4.1. Overall Energetic Performance

The oxidative current was less than 0.1 A m^{-2} during all chronoamperometries (Figure 1) within the first two days of polarization for the negative potential, and five days for the positive one. In addition, during all voltamperometries performed at day 0 for both polarization potentials (data not published). This indicates that the microbial community carried in the inoculum did not have the adequate conditions to deliver electrons to the anode right away, suggesting that, in order to produce current, some microbes need to be selected at the anode surface, and some microbes need to grow and produce redox mediators in the liquid fraction during the adaptation period [44].

Tendencies in current density during all the experiment and its values were similar to the results obtained by Dominguez-Benetton et al. [10], who evaluate a marine biofilm-supported carbon cloth (25 cm^2) in a three-electrode set-up (polarization at +0.34 V/SHE) employing synthetic media (49 mS cm^{-1}). As in this study, the mean current density was about 1.00 to 2.00 A m^{-2} . Peak values were superior during chronoamperometry in comparison to this work (up to 3.50 A m^{-2}), although the electrolytic conductivity used here was 1.4 times higher ($67.12 \pm 2.84 \text{ mS cm}^{-1}$). The same inoculum was previously studied by Erable and Bergel [18], providing up to 4 A m^{-2} for 10 mM acetate oxidation at +0.14 V/SHE, when a stainless steel sheet was used as the supporting material. However, modest current densities were observed at replicates (max. of 1.1, 1.2, 2.2, and 3.1 A m^{-2}), showing some variability as well. These current densities were normalized with respect to the cathode area, which was 0.8 times the anode area. Higher values were reported in the same work when the anode supporting material was substituted with plain graphite (5.9 A m^{-2}) and a stainless steel grid (8.2 A m^{-2}), indicating that, despite large variability, the selected anodic collector seems to be crucial to enhance current outputs. Albeit the lower maximum current densities achieved here, similar performance was observed. Thus, microbial communities and the effect of the anodic collector would be interesting to address in future studies, as the bioanodes obtained in this work seem to behave like marine bioanodes, but with a more conductive electrolyte.

By contrast, Rousseau et al. [7] used salt marsh sediments (76 – 123 mS cm^{-1}) as the inoculum source in a three-electrode arrangement with a carbon felt electrode (2 cm^2) as working electrode (polarization at +0.34 V/SHE). Despite the fact that the inoculum type, cell configuration, polarization potential, materials, and electrolyte (70 mS cm^{-1}) were mostly identical to this work, the maximal current densities reported here are less significant (2.64 A m^{-2}) than those obtained by Rousseau et al. [7] (16, 50, and 65 A m^{-2} per replicate). However, the ratio between working volume and anode projected area was about nine times greater, which may explain why the maximal current densities were far superior compared to this work, as carbon source depletion near the electrochemically active surface is less likely to occur. It is noteworthy that elevated current outputs were not quite reproducible in a further study conducted at different polarization potentials, even though the electrolyte conductivity was more elevated (104 mS cm^{-1}) in comparison to this report and a large volume versus area ratio was conserved [8]. Maximum current densities were of 1.00, 2.50, 2.50, 5.00, and 8.00 A m^{-2} at -0.16 V/SHE ; 5.00, 7.00, 8.00, 12.00, and 31 A m^{-2} at +0.24 V/SHE; plus 7.00, 8.00, 24.00, 26.00, and 39.00 A m^{-2} at +0.44 V/SHE, which are modest compared to the previous study [7] and closer to the values reported here (Table 1).

In accordance with other authors [7,8], high variability between replicates is observed, as is expected for large inoculum sizes. The heterogeneity in composition that is inherent to the sediments [50], plus the large size of the inoculum, are likely the key reason [7], as a result of the presence of a high variety of chemical species and their concentration within the sediments and hence in the electrochemical cell after inoculation. Sulfate is a common ion in marine and haline lagoon sediments, directly contributing to the sulfate-reducing activity and sulfide production [51], and impacting on current generation [52]. Also, the relatively low and variable coulombic efficiencies obtained in this work, in agreement with others reported when salt marsh sediments are used as the inoculum source in large proportions [7,8], may be explained by the sulfate-reducing activity, because six of the eight electrons employed to reduce sulfate are wasted, i.e., the electrochemical oxidation of sulfide yields only two electrons per mole of acetate as opposed to eight electrons from the direct exoelectrogenic conversion using the anode as an electron sink [44,53,54]. Thus, the influence of sulfate concentration on current production and coulombic efficiency when large inoculum sizes are employed should be more carefully addressed in further studies. Additionally, iron, a solid respiratory-chain electron acceptor of many exoelectrogenic bacteria, such as *Geobacteraceae* [55], is also a common element in marine sediments [50,55] that may compete with the anodic reactions for the electrons harnessed by the exoelectrogenic community from the carbon source [7], contributing to the low coulombic efficiencies and the high variability between replicates when large amounts of sediments are used as inoculum in MES. Such conditions may favor the establishment of a planktonic (suspended) microbial community that may or may not be electrochemically active.

In a similar work, Doyle et al. [29] employed sediments of a highly saline artificial hydric system ($100\text{--}750\text{ mS cm}^{-1}$) for bioanode development at polarization potentials of +0.40 and +0.60 V/SHE, producing a maximum current density of 5.2 and 4.8 A m^{-2} , respectively. These values were more modest than those obtained by Rousseau et al. [7], but more consistent with those found here. Such a difference may be explained by *Geobacter* dominant species found by Doyle et al. [29], which are often reported in marine and freshwater MES [37,46,56], whereas Rousseau et al. [7,27] found *Desulfuromonas* spp. and *Marinobacter* spp. as dominant species, of which the former are more typical of marine environments, while the latter were reported for the first time as an important species for current production. A further 16S rDNA gene assessment will be necessary to determine whether the similarities between the current density values found here and those found by other authors are due to anode-colonizing microbiota, and also to clarify the role of the suspended community.

4.2. Implications of Polarization Potential for Current Density

As has been demonstrated in several works (including this one), a high variability in current density is usually observed when marine and saline inocula are used to grow bioanodes because a large amount (10 vol % to 50 vol %) is commonly employed [7,8,10,18,27,29,30,42,44]. This is important to take into account when conclusions about the effect of polarization potential over current density are made since several replicates, and statistical analysis, are not usually addressed [29,30,33,36]. In this work, it was observed that higher polarization potentials might offer advantages, like better organic matter removal. However, higher polarization potentials do not seem to affect current output significantly in comparison with lower potentials, at least with the inoculum and experimental conditions used here. Thus, current production may be more dependent on other factors besides the applied potential [37,56]. This may be true because, according to the literature, the main genera colonizing the anode surface do not vary with the applied potential, but their abundance does, indicating that the selected species are more influenced by the inoculum itself, and only slight differences in its proportion are governed by polarization potential [8,36]. Of course, further analysis of the bioanode microbial community growth in this study is still needed to elucidate this issue. Remarkably, a lower polarization potential seems to enhance some electrochemical parameters, as has been previously reported [8,42], which is in accordance with the higher coulombic efficiencies reported here when a negative polarization potential was applied. Differences between experimental designs

must be considered in order to understand the role of the applied potential over the enriched microbial species and the community structure, and its relationship with current density. Torres et al. [36] found that a negative potential (-0.15 V/SHE) yielded better current densities because of a stringent selection of *Geobacter* spp. (97% of abundance); it is noteworthy that the bioanode enrichment was made in the same vessel along with the other three bioanodes polarized at -0.09 V/SHE, $+0.02$ V/SHE, and $+0.37$ V/SHE. These results contradict those reported by Rousseau et al. [8], where positive potentials were more beneficial no matter if the electrodes were polarized at different potentials within the same cell (-0.06 V/SHE, $+0.14$ V/SHE, $+0.24$ V/SHE, and $+0.44$ V/SHE), resulting in a stringent selection of *Marinobacter* spp. and *Desulfuromonas* spp. The main differences between the two cited reports were the inoculum source and size (wastewater and sludge, 2 vol % vs. salt marsh sediment, 10 vol %), media composition and conductivity (fresh water vs. highly saline electrolyte), feeding regime (unagitated batch without starvation vs. continuous flow) and collector porosity (plain graphite vs. felt), suggesting that the inoculum, electrolyte composition, and collector properties play an important role with respect to which species are selected under different applied potentials, as was pointed out by Commault et al. [38]. Another important difference was the length of those studies in comparison with ours; these previous studies evolve way beyond the peak current achieved in the system, whereas in our case we barely achieved this stage. This aspect is typically related to the variability in diversity and structure of the microbial community, which, beyond peak current, is governed by the geochemical environment [45]. Our results also indicate that polarization potential has no effect on overall current output despite the applied polarization potential during biofilm growth, as the maximum current density obtained in all the experiments was a function of the applied overvoltage during voltammetry and similar peaks were found for both applied potentials (Figure 3). The peaks observed in the voltammograms obtained in this work seem to be characteristic of *Geobacter* species (low overvoltages) obtained at negative polarization potential (-0.15 V/SHE), but also of species from other families such as *Pseudomonadales* (high overvoltages), enriched at higher polarization potentials ($+0.37$ V/SHE), according to results obtained by Torres et al. [36]. This indicates that, in our case, both polarization potentials applied during bioanode growth allowed the enrichment of similar communities—but presumably they were not fully mature at the final stage of experimentation. This issue should be addressed in further studies by 16S rRNA gene and cyclic voltammetry first derivative analysis of the enriched community. Also, it is important to recognize that longer operation terms and a continuous-flow regime, as well as other techniques to remove non-exoelectrogenic bacteria from the system (i.e., chemical inhibitors and shearing) [36,57] may lead to higher current outputs than the ones observed here. This idea is supported by Ichihashi et al. [57], who achieved large increments in current density (2.3 to 38.4 A m⁻²) and coulombic efficiency (50% to 80%) by employing a continuous-flow operation system with successive organic loading rate increments, and removing the excess of biomass by flushing the anode chamber at high shear rates (>30 mL min⁻¹), as an enrichment technique. It is worth mentioning that, with this technique [57], the variability in current output between replicates was presumably reduced after 26 to 29 days of operation, suggesting that this approach would be interesting to address in the future in order to enhance the energetic performance of halotolerant bioanodes and avoid a lack of reproducibility. Therefore, to enhance the anode current production of halotolerant bioanodes, other subjects like the anode collector [18,44], volume versus anode area ratio [7,8,27], microorganism source and inoculum size [38], electrolyte composition [7,10], electrode materials [18,44], substrate type and concentration feeding regime [57], batch and continuous flow operation, and length of the experiment [38,57] must be taken into account, as they seem to impact current output in a more significant way than applied polarization potential during bioanode growth, when practical applications are considered. Also, the contributions of the suspended and electrode microbial community to current production and coulombic efficiency should be carefully addressed in the future.

Acknowledgments: The authors thank the “Consejo Nacional de Ciencia y Tecnología” (CONACYT grant no. 421498) and CEMIE-Biogas-SENER, in México, for the financial support. Also, the authors thank to Manuel Aguilar-Vega and to the “Laboratorio de Membranas” (CICY) for providing the facilities to perform the experiments.

Author Contributions: Muriel González-Muñoz wrote the manuscript, designed and performed the experiments; Xochitl Dominguez-Benetton contributed the main ideas for the experiments, discussed the experimental results, and helped edit the manuscript; Jorge Domínguez-Maldonado and David Valdés-Lozano performed the sediment and water recollection and analysis, helped with technical support during the experiments, and provided materials and instruments to perform the chemical analysis; Daniella Pacheco-Catalán helped design the electrochemical experiments and provided materials to perform the experiments; Otto Ortega-Morales provided technical support in the microbiology area; Liliana Alzate-Gaviria conceived, led, financed, and supervised the study, and edited the manuscript.

Conflicts of Interest: The authors declare no conflict of interest.

References

1. Logan, B.E.; Rabaey, K. Conversion of Wastes into Bioelectricity and Chemicals by Using Microbial Electrochemical Technologies. *Science* **2012**, *337*, 686–690. [[CrossRef](#)] [[PubMed](#)]
2. Zhang, Y.; Irini, A. Microbial Electrolysis Cells Turning to Be Versatile Technology: Recent Advances and Future Challenges. *Water Res.* **2014**, *56*, 11–25. [[CrossRef](#)] [[PubMed](#)]
3. Luo, H.; Liu, G.; Zhang, R.; Bai, Y.; Fu, S.; Hou, Y. Heavy Metal Recovery Combined with H₂ Production from Artificial Acid Mine Drainage Using the Microbial Electrolysis Cell. *J. Hazard. Mater.* **2014**, *270*, 153–159. [[CrossRef](#)] [[PubMed](#)]
4. Wang, H.; Ren, Z.J. Bioelectrochemical Metal Recovery from Wastewater: A Review. *Water Res.* **2014**, *66*, 219–232. [[CrossRef](#)] [[PubMed](#)]
5. Dominguez-Benetton, X.; Chandrakant-Varia, J.; Pozo, G.; Modin, O.; Ter Heijne, A.; Fransaer, J.; Rabaey, K. Metal Recovery by Microbial Electro-Metallurgy. *Prog. Mater. Sci.* **2018**, *94*, 435–461. [[CrossRef](#)]
6. Dominguez-Benetton, X.; Seveda, S.; Vanbroekhoven, K.; Pant, D. The Accurate Use of Impedance Analysis for the Study of Microbial Electrochemical Systems. *Chem. Soc. Rev.* **2012**, *41*, 7228–7246. [[CrossRef](#)] [[PubMed](#)]
7. Rousseau, R.; Dominguez-Benetton, X.; Délia, M.L.; Bergel, A. Microbial Bioanodes with High Salinity Tolerance for Microbial Fuel Cells and Microbial Electrolysis Cells. *Electrochem. Commun.* **2013**, *33*, 1–4. [[CrossRef](#)]
8. Rousseau, R.; Santaella, C.; Bonnafous, A.; Achouak, W.; Godon, J.J.; Delia, M.L.; Bergel, A. Halotolerant Bioanodes: The Applied Potential Modulates the Electrochemical Characteristics, the Biofilm Structure and the Ratio of the Two Dominant Genera. *Bioelectrochemistry* **2016**, *112*, 24–32. [[CrossRef](#)] [[PubMed](#)]
9. Lacroix, R.; Da Silva, S.; Gaig, M.V.; Rousseau, R.; Delia, M.L.; Bergel, A. Modelling Potential/Current Distribution in Microbial Electrochemical Systems Shows How the Optimal Bioanode Architecture Depends on Electrolyte Conductivity. *Phys. Chem. Chem. Phys.* **2014**, *16*, 22892–22902. [[CrossRef](#)] [[PubMed](#)]
10. Dominguez-Benetton, X.; Godon, J.J.; Rousseau, R.; Erable, B.; Bergel, A.; Délia, M.L. Exploring Natural vs. Synthetic Minimal Media to Boost Current Generation with Electrochemically-Active Marine Bioanodes. *J. Environ. Chem. Eng.* **2016**, *4*, 2362–2369. [[CrossRef](#)]
11. Feng, Y.; Wang, X.; Logan, B.E.; Lee, H. Brewery Wastewater Treatment Using Air-Cathode Microbial Fuel Cells. *Appl. Microbiol. Biotechnol.* **2008**, *78*, 873–880. [[CrossRef](#)] [[PubMed](#)]
12. Lefebvre, O.; Quentin, S.; Torrijos, M.; Godon, J.J.; Delgenes, J.P.; Moletta, R. Impact of Increasing NaCl Concentrations on the Performance and Community Composition of Two Anaerobic Reactors. *Appl. Microbiol. Biotechnol.* **2007**, *75*, 61–69. [[CrossRef](#)] [[PubMed](#)]
13. Lefebvre, O.; Tan, Z.; Kharkwal, S.; Ng, H.Y. Effect of Increasing Anodic NaCl Concentration on Microbial Fuel Cell Performance. *Bioresour. Technol.* **2012**, *112*, 336–340. [[CrossRef](#)] [[PubMed](#)]
14. Liu, H.; Cheng, S.; Logan, B.E. Power Generation in Fed-Batch Microbial Fuel Cells as a Function of Ionic Strength, Temperature, and Reactor Configuration. *Environ. Sci. Technol.* **2005**, *39*, 5488–5493. [[CrossRef](#)] [[PubMed](#)]
15. De Schamphelaire, L.; Rabaey, K.; Boeckx, P.; Boon, N.; Verstraete, W. Outlook for Benefits of Sediment Microbial Fuel Cells with Two Bio-Electrodes. *Microbiol. Biotechnol.* **2008**, *1*, 446–462. [[CrossRef](#)] [[PubMed](#)]

16. Xu, X.; Zhao, Q.; Wu, M.; Ding, J.; Zhang, W. Biodegradation of Organic Matter and Anodic Microbial Communities Analysis in Sediment Microbial Fuel Cells with/without Fe(III) Oxide Addition. *Bioresour. Technol.* **2017**, *225*, 402–408. [[CrossRef](#)] [[PubMed](#)]
17. Zhao, Q.; Li, R.; Ji, M.; Ren, Z.J. Organic Content Influences Sediment Microbial Fuel Cell Performance and Community Structure. *Bioresour. Technol.* **2016**, *220*, 549–556. [[CrossRef](#)] [[PubMed](#)]
18. Erable, B.; Bergel, A. First Air-Tolerant Effective Stainless Steel Microbial Anode Obtained from a Natural Marine Biofilm. *Bioresour. Technol.* **2009**, *100*, 3302–3307. [[CrossRef](#)] [[PubMed](#)]
19. Monzon, O.; Yang, Y.; Yu, C.; Li, Q.; Alvarez, P.J.J. Microbial Fuel Cells under Extreme Salinity: Performance and Microbial Analysis. *Environ. Chem.* **2014**, *12*, 293–299. [[CrossRef](#)]
20. Oren, A. Microbial Life at High Salt Concentrations: Phylogenetic and Metabolic Diversity. *Saline Syst.* **2008**, *4*, 2. [[CrossRef](#)] [[PubMed](#)]
21. Oren, A. Life at High Salt Concentrations. In *The Prokaryotes: Prokaryotic Communities and Ecophysiology*; Rosenberg, E., DeLong, E.F., Lory, S., Stackebrandt, E., Thompson, F., Eds.; Springer: Berlin/Heidelberg, Germany, 2013; pp. 421–440.
22. Weyl, P.K. On the Change in Electrical Conductance of Seawater with Temperature 1. *Limnol. Oceanogr.* **1964**, *9*, 75–78. [[CrossRef](#)]
23. DasSarma, S.; DasSarma, P. Halophiles. In *eLS*; John Wiley & Sons: Hoboken, NJ, USA, 2001.
24. Pol, L.W.; Lens, P.N.; Weijma, J.; Stams, A.J. New Developments in Reactor and Process Technology for Sulfate Reduction. *Water Sci. Technol.* **2001**, *44*, 67–76. [[PubMed](#)]
25. Santoro, C.; Arbizzani, C.; Erable, B.; Ieropoulos, I. Microbial Fuel Cells: From Fundamentals to Applications. A Review. *J. Power Sources* **2017**, *356*, 225–244. [[CrossRef](#)] [[PubMed](#)]
26. Schroder, U. Anodic Electron Transfer Mechanisms in Microbial Fuel Cells and Their Energy Efficiency. *Phys. Chem. Chem. Phys.* **2007**, *9*, 2619–2629. [[CrossRef](#)] [[PubMed](#)]
27. Rousseau, R.; Santaella, C.; Achouak, W.; Godon, J.J.; Bonnafous, A.; Bergel, A.; Délia, M.L. Correlation of the Electrochemical Kinetics of High-Salinity-Tolerant Bioanodes with the Structure and Microbial Composition of the Biofilm. *ChemElectroChem* **2014**, *1*, 1966–1975. [[CrossRef](#)]
28. Abrevaya, X.C.; Sacco, N.; Mauas, P.J.D.; Cortón, E. Archaea-Based Microbial Fuel Cell Operating at High Ionic Strength Conditions. *Extremophiles* **2011**, *15*, 633–642. [[CrossRef](#)] [[PubMed](#)]
29. Doyle, L.E.; Yung, P.Y.; Mitra, S.D.; Wuertz, S.; Williams, R.B.H.; Lauro, F.M.; Marsili, E. Electrochemical and Genomic Analysis of Novel Electroactive Isolates Obtained Via Potentiostatic Enrichment from Tropical Sediment. *J. Power Sources* **2017**, *356*, 539–548. [[CrossRef](#)]
30. Grattieri, M.; Suvira, M.; Hasan, K.; Minteer, S.D. Halotolerant Extremophile Bacteria from the Great Salt Lake for Recycling Pollutants in Microbial Fuel Cells. *J. Power Sources* **2017**, *356*, 310–318. [[CrossRef](#)]
31. Holmes, D.E.; Bond, D.R.; O’Neil, R.A.; Reimers, C.E.; Tender, L.R.; Lovley, D.R. Microbial Communities Associated with Electrodes Harvesting Electricity from a Variety of Aquatic Sediments. *Microb. Ecol.* **2004**, *48*, 178–190. [[CrossRef](#)] [[PubMed](#)]
32. Monzon, O.; Yang, Y.; Kim, J.; Heldenbrand, A.; Li, Q.; Alvarez, P.J.J. Microbial Fuel Cell Fed by Barnett Shale Produced Water: Power Production by Hypersaline Autochthonous Bacteria and Coupling to a Desalination Unit. *Biochem. Eng. J.* **2017**, *117*, 87–91. [[CrossRef](#)]
33. Finkelstein, D.A.; Tender, L.M.; Zeikus, J.G. Effect of Electrode Potential on Electrode-Reducing Microbiota. *Environ. Sci. Technol.* **2006**, *40*, 6990–6995. [[CrossRef](#)] [[PubMed](#)]
34. Sun, D.; Cheng, S.; Zhang, F.; Logan, B.E. Current Density Reversibly Alters Metabolic Spatial Structure of Exoelectrogenic Anode Biofilms. *J. Power Sources* **2017**, *356*, 566–571. [[CrossRef](#)]
35. Lewis, A.J.; Borole, A.P. Adapting Microbial Communities to Low Anode Potentials Improves Performance of Mecs at Negative Potentials. *Electrochim. Acta* **2017**, *254*, 79–88. [[CrossRef](#)]
36. Torres, C.I.; Krajmalnik-Brown, R.; Parameswaran, P.; Marcus, A.K.; Wanger, G.; Gorby, Y.A.; Rittmann, B.E. Selecting Anode-Respiring Bacteria Based on Anode Potential: Phylogenetic, Electrochemical, and Microscopic Characterization. *Environ. Sci. Technol.* **2009**, *43*, 9519–9524. [[CrossRef](#)] [[PubMed](#)]
37. Zhu, X.; Yates, M.D.; Hatzell, M.C.; Rao, H.A.; Saikaly, P.E.; Logan, B.E. Microbial Community Composition Is Unaffected by Anode Potential. *Environ. Sci. Technol.* **2014**, *48*, 1352–1358. [[CrossRef](#)] [[PubMed](#)]
38. Commault, A.S.; Lear, G.; Packer, M.A.; Weld, R.J. Influence of Anode Potentials on Selection of Geobacter Strains in Microbial Electrolysis Cells. *Bioresour. Technol.* **2013**, *139*, 226–234. [[CrossRef](#)] [[PubMed](#)]

39. Wagner, R.C.; Call, D.F.; Logan, B.E. Optimal Set Anode Potentials Vary in Bioelectrochemical Systems. *Environ. Sci. Technol.* **2010**, *44*, 6036–6041. [[CrossRef](#)] [[PubMed](#)]
40. Babauta, J.; Renslow, R.; Lewandowski, Z.; Beyenal, H. Electrochemically active biofilms: Facts and fiction. A review. *Biofouling* **2012**, *28*, 789–812. [[CrossRef](#)] [[PubMed](#)]
41. American Public Health Association (APHA). *Standard Methods of Water and Wastewater*; American Public Health Association; American Water Works Association; Water Environment Federation Publication: Washington, DC, USA, 1996.
42. Rousseau, R.; Rimboud, M.; Délia, M.L.; Bergel, A.; Basséguy, R. Electrochemical Characterization of Microbial Bioanodes Formed on a Collector/Electrode System in a Highly Saline Electrolyte. *Bioelectrochemistry* **2015**, *106*, 97–104. [[CrossRef](#)] [[PubMed](#)]
43. Wolfe, R.S. Techniques for Cultivating Methanogens. *Methods Enzymol.* **2011**, *494*, 1–22. [[PubMed](#)]
44. Erable, B.; Roncato, M.A.; Achouak, W.; Bergel, A. Sampling Natural Biofilms: A New Route to Build Efficient Microbial Anodes. *Environ. Sci. Technol.* **2009**, *43*, 3194–3199. [[CrossRef](#)] [[PubMed](#)]
45. White, H.K.; Reimers, C.E.; Cordes, E.E.; Dilly, G.F.; Girguis, P.R. Quantitative population dynamics of microbial communities in plankton-fed microbial fuel cells. *ISME J.* **2009**, *3*, 635–646. [[CrossRef](#)] [[PubMed](#)]
46. Logan, B.E. Microbial Fuel Cells: Methodology and Technology. *Environ. Sci. Technol.* **2006**, *40*, 5181–5192. [[CrossRef](#)] [[PubMed](#)]
47. Logan, B.E. *Microbial Fuel Cells*; Wiley-Interscience: Hoboken, NJ, USA, 2008.
48. Wang, X.; Feng, Y.; Ren, N.; Wang, H.; Lee, H.; Li, N.; Zhao, Q. Accelerated Start-up of Two-Chambered Microbial Fuel Cells: Effect of Anodic Positive Poised Potential. *Electrochim. Acta* **2009**, *54*, 1109–1114. [[CrossRef](#)]
49. Heijne, A.T.; Liu, F.; Weijden, R.; Weijma, J.; Buisman, C.J.; Hamelers, H.V. Copper Recovery Combined with Electricity Production in a Microbial Fuel Cell. *Environ. Sci. Technol.* **2010**, *44*, 4376–4381. [[CrossRef](#)] [[PubMed](#)]
50. Libes, S. *Introduction to Marine Biogeochemistry*, 2nd ed.; John Wiley and Sons: Hoboken, NJ, USA, 2009; 1715p, ISBN 9780120885305.
51. Valdes, D.; Real, E. Nitrogen and Phosphorus in Water and Sediments at Ria Lagartos Coastal Lagoon, Yucatan, Gulf of Mexico. *Indian J. Mar. Sci.* **2004**, *33*, 338–345.
52. Rabaey, K.; Van de Sompel, K.; Maignien, L.; Boon, N.; Aelterman, P.; Clauwaert, P.; De Schampelaire, L.; Pham, H.T.; Vermeulen, J.; Verhaege, M.; et al. Microbial Fuel Cells for Sulfide Removal. *Environ. Sci. Technol.* **2006**, *40*, 5218–5224. [[CrossRef](#)] [[PubMed](#)]
53. Lovley, D.R. Microbial Fuel Cells: Novel Microbial Physiologies and Engineering Approaches. *Curr. Opin. Biotechnol.* **2006**, *17*, 327–332. [[CrossRef](#)] [[PubMed](#)]
54. Muyzer, G.; Stams, A.J. The Ecology and Biotechnology of Sulphate-Reducing Bacteria. *Nat. Rev. Microbiol.* **2008**, *6*, 441–454. [[CrossRef](#)] [[PubMed](#)]
55. Lovley, D.R. Bug Juice: Harvesting Electricity with Microorganisms. *Nat. Rev. Microbiol.* **2006**, *4*, 497–508. [[CrossRef](#)] [[PubMed](#)]
56. Zhu, X.; Yates, M.D.; Hatzell, M.C.; Rao, H.A.; Saikaly, P.E.; Logan, B.E. Response to Comment on Microbial Community Composition Is Unaffected by Anode Potential. *Environ. Sci. Technol.* **2014**, *48*, 14853–14854. [[CrossRef](#)] [[PubMed](#)]
57. Ichihashi, O.; Vishnivetskaya, T.A.; Borole, A.P. High-Performance Bioanode Development for Fermentable Substrates via Controlled Electroactive Biofilm Growth. *ChemElectroChem* **2014**, *1*, 1940–1947. [[CrossRef](#)]

